



# RESEARCH MEMORANDUM

EXPERIMENTAL INVESTIGATION OF EFFECT OF JET EXIT  
CONFIGURATION ON THRUST AND DRAG

By Edmund E. Callaghan and Willard D. Coles

Lewis Flight Propulsion Laboratory  
Cleveland, Ohio

NATIONAL ADVISORY COMMITTEE  
FOR AERONAUTICS

WASHINGTON  
December 20, 1951

## NATIONAL ADVISORY COMMITTEE FOR AERONAUTICS

RESEARCH MEMORANDUM

## EXPERIMENTAL INVESTIGATION OF EFFECT OF JET EXIT

## CONFIGURATION ON THRUST AND DRAG

By Edmund E. Callaghan and Willard D. Coles

## SUMMARY

The problem of performance losses occurring when airplanes equipped with afterburner and cooling-air ejector installations are flown with the afterburner inoperative has been experimentally investigated in a wind tunnel. The modification of the basic (nonejecting) configuration to an ejector configuration was accomplished without any large increase in the drag of the body. At low values of the ratio of cooling-air flow to propulsive jet flow, overexpansion and attachment of the jet to the ejector shroud ring with a consequent internal shock system was found to be one source of performance loss. Reduction of the nozzle area with the afterburner inoperative so changes the characteristics of the ejector that excessive pumping action of the ejector may result in large internal pressure losses. The excessive pumping action occurring under such off-design operating conditions is a more probable cause of the performance loss than the internal shock system resulting from operation at low values of cooling-air flow ratio.

The effect of a partial shroud on jet thrust appears negligible as long as the jet remains unattached. The results indicate that, for the model investigated, attachment of the jet appears likely at high jet pressure ratios.

## INTRODUCTION

The usual means of increasing the performance of a jet-powered aircraft with minimum modification is by the installation of an afterburner. One of the requirements of an afterburner installation is an adequate supply of cooling air to maintain the afterburner inside skin temperature at a safe level. The afterburner cooling air is normally obtained by utilizing the ejector principle. The propulsive jet is discharged through a shroud and thereby creates a region of low pressure, which is used to pump the required cooling air flow.

Recent flight experiences with aircraft modified in this manner have shown that, although the aircraft performance could be increased by

afterburning, large performance losses occurred at cruise speeds with the afterburner inoperative. For such a condition, the exit nozzle would normally be in a closed position and an entirely different ejector configuration than that used with afterburning would result. The loss in performance must be caused by either a decrease in net thrust or an increase in base drag. Net thrust losses might occur because of excessive pumping of cooling air or internal flow phenomena, which reduce the jet thrust. An increase in base drag might be caused by incomplete filling of the jet exit by the jet. An investigation was therefore initiated at the NACA Lewis laboratory to determine the source of the losses.

The experimental investigation was conducted with similar models of various exit configurations of current interest in the 6- by 9-foot test section of the Lewis icing research tunnel. Air for the jet was ducted to the model at relatively low temperatures with pressures ranging up to 4 atmospheres. The model was investigated first without an afterburner and then modified to simulate an installation with an afterburner. These modifications consisted of internal changes to represent exits with two different ejectors. The only external difference between the original model and the modified exits was a slight increase in the over-all base diameter.

The ejector configurations investigated were designed to simulate the flight-condition geometry which resulted in performance loss. Hence, the ejector shroud diameter was based on that required to obtain a normal cooling air flow of 5 percent of the jet air-flow rate at the design conditions with afterburning and the nozzle-exit diameter was that used for nonafterburning operation.

An additional configuration, which was also investigated, consisted of a semishrouded exit and tail boom. No cooling air was used with this configuration and it was investigated primarily to study the pressure effect of the jet on a semishroud and possible performance losses resulting from such shrouding.

Each model was investigated over a range of over-all jet pressure ratios (ratio of jet total pressure to stream static pressure) of 2.0 to 4.0 for a range of tunnel velocities from 0 to 500 feet per second. Cooling air was varied over a range from 0 to 10 percent of the jet air-flow rate.

#### SYMBOLS

The following symbols are used in this report:

$P_b$  cooling-air total pressure (lb/sq ft)

$P_j$  jet total pressure (lb/sq ft)

$p_x$  surface static pressure (lb/sq ft)  
 $p_0$  stream static pressure (lb/sq ft)  
 $q_0$  free-stream dynamic pressure (lb/sq ft)  
 $P_0$  free-stream total pressure (lb/sq ft)

#### APPARATUS AND PROCEDURE

The investigation was made using a streamlined body of revolution,  $\frac{3}{4}$  feet long, 1 foot in diameter at the largest section, mounted in the 6- by 9-foot test section of the icing research tunnel as shown in figure 1. The model had a wooden nose section, a center section of constant diameter, and a rear section which could be readily altered for the various modifications. Details of the tunnel installation and of the model are shown in figure 2. Internally the model consists of a cylindrical midsection, a nozzle tube simulating a tail pipe or after-burner, and a conical nozzle. The model was mounted to the tunnel scale system by means of a heavy rectangular duct section, which also served as a passage for the jet air. The rectangular model support was enclosed in a streamlined fairing to minimize the aerodynamic forces acting on the supporting section and to permit the measurement of thrust and drag forces acting on the body.

Cooling air was passed through the annulus formed by the nozzle tube and the outer fairing for the configurations in which cooling-air flow was to be simulated. The schematic diagram of the installation also shows the method employed to isolate the thrust and aerodynamic forces on the model from the piping system, and to isolate the pressure and flow forces on the piping system from the model. Two rubber expansion joints in the vertical riser of the 6-inch jet-air supply line which were restrained longitudinally by tie rods with ball bearing ends, and two vertical pieces of rubber hose in a U-tube arrangement in the cooling-air supply line successfully isolated the model from the piping so that thrust and drag measurements could be obtained.

Four variations of the basic model were investigated and were designated as configurations I to IV (fig. 3). Differences among the configurations were confined to the nozzle tube and other portions of the rear section of the model. The nose section and the midsection of the model remained unchanged throughout the investigation. All the configurations had similar  $15^\circ$  converging jet-nozzle tubes with length the only variable among nozzle tubes. All exit nozzles were of  $3.000 \pm 0.002$  inch diameter and had nozzle tube inside diameters of 5.05 inches.

Configuration I (fig. 3(a)) was designed to simulate a jet engine without afterburner. The nozzle tube fitted into the shell of the outer fairing with no clearance and thus there was no provision for passing cooling air between the outer fairing and the nozzle tube.

Configurations II and III consisted of modifications to the basic model and simulated a jet-engine installation modified to include an afterburner. For these configurations, 13/32 inch was cut off the rear portion of the outer fairing to provide the opening required for the passage of cooling air between the nozzle tube and the outer fairing.

Configuration II (fig. 3(b)) had the nozzle tube exhausting into an annular shroud ring thereby causing an ejector action for the cooling air. The dimensions of the shroud ring were such that with afterburning the ejector would pump cooling air at a rate of 5 percent jet-air flow rate at 30,000 feet and a flight Mach number of 0.9 with ram air. The jet nozzle diameter, however, was that which would occur with no afterburning, thus simulating the off-design condition for the ejector which had resulted in the performance losses experienced in flight. Configuration II was therefore constructed with a jet diameter of 3 inches, a shroud diameter of 3.77 inches, and a shroud length of 0.72 inch.

Configuration III (fig. 3(c)) also simulated operation with the conditions under which loss of performance in flight had occurred. A long annular shroud ring was used which was designed to pump cooling air at a rate of 5 percent jet-air flow rate at sea-level, take-off conditions with afterburning, and the nozzle diameter was that which the engine would require when the afterburner was inoperative. Configuration III had the same jet and shroud diameter as configuration II, but a shroud length of 1.79 inches.

Configuration IV (fig. 3(d)) was essentially the same as configuration I, with a partial shroud and tail boom over the exit of the jet to simulate a jet-engine installation with the jet partly confined under the tail assembly of the airplane.

Instrumentation of the model is shown in figure 2 and consisted of thermocouples to measure jet- and cooling-air temperatures, static-pressure taps along the top surface of the rear section of the outer shell, total-pressure tubes in the nozzle tube ahead of the exit, and shielded total-pressure tubes in the cooling-air passage between the nozzle tube and the outer shell. Configuration IV had, in addition, static taps along the inside top surface of the shroud and tail-boom portion (fig. 4).

Orifices in the air supply lines to the jet- and cooling-air systems were used to measure the flow of air in the two systems.

Each configuration was investigated for a range of pressure ratio from approximately 2.0 to 4.0 at tunnel velocities of 0, 220, 305, 380, 440, and 500 feet per second. For configurations II and III, the cooling-air

flow rate was varied from 0 to 10 percent of the jet flow rate at fixed values of tunnel-air velocity and jet pressure ratio. The jet-air temperature was approximately 160° F and the cooling-air temperature was approximately 50° F for the entire investigation. Tunnel-air temperature varied from 50° to 90° F.

### RESULTS AND DISCUSSION

The ejector configurations used in this investigation were designed to simulate the condition encountered by an airplane equipped with an afterburner but flying with the afterburner inoperative. Under such conditions the exit nozzle would be in a closed position and the ratio of the shroud area to the jet exit area would be large. The performance losses cited previously undoubtedly result from such off-design operation and are caused by a decrease in jet thrust, an increase in base drag, or internal duct pressure losses due to excessive pumping.

A comparison of the jet thrust and jet thrust-minus-drag characteristics of configuration I with those of the other configurations should reveal any large losses in thrust or increases in base drag.

One means of comparing the results is in terms of the ratio of the thrust minus drag of the ejector configuration to that of configuration I. This ratio is plotted as a function of the over-all jet pressure ratio  $P_j/p_0$  for constant values of the cooling-air flow ratio (ratio of cooling-air flow to jet-air flow) and at a particular tunnel-air velocity. Such a comparison is shown in figure 5 for configuration II at cooling-air flow ratios of 0, 0.04, and 0.08 for a tunnel velocity of 305 feet per second.

These curves were obtained by plotting the jet thrust minus drag of configuration II at the particular tunnel velocity as a function of the cooling-air flow ratio for constant values of the jet pressure ratio. From curves such as these and a plot of the jet thrust minus drag as a function of jet pressure ratio for configuration I, the curves shown in figure 5 are easily obtained. The data at all the other tunnel-air velocities investigated were analyzed in the same manner and curves the same as those shown in figure 5 were obtained. The effect of stream velocity therefore appears to be negligible. In addition, the surface pressure distribution measured on the rear top surface of the outer shell was studied in terms of the pressure coefficient  $\left(1 - \frac{p_x - p_0}{q_0}\right)$  and found to

be nearly the same for all values of jet pressure ratio, cooling-air flow, and tunnel-air velocity. This distribution would indicate that the body drag coefficient was therefore independent of jet pressure ratio, cooling-air flow, and tunnel-air velocity. The slight increase in the thrust-minus-drag ratio with increasing pressure ratio probably results

from expansion of the jet to a static pressure close to atmospheric before discharge from the shroud into the atmosphere. In this manner, nearly isentropic expansion of the jet occurs and, hence, a slight increase in thrust. The increase in thrust-minus-drag ratio with increasing cooling-air flow ratio is expected and results from the mass of cooling air being discharged at a finite velocity. This additional momentum also accounts for the values of thrust-minus-drag ratio greater than unity shown in figure 5.

The thrust-minus-drag ratio for zero cooling-air flow is always less than unity for the range of jet pressure ratios shown. Because these are data for zero tunnel-air velocity, also, that is, zero drag, it is obvious that the thrust of configuration II is less than that of configuration I for all values of pressure ratio. Because the curves of thrust-minus-drag ratio were found to be the same for all values of tunnel velocity including zero, apparently no large increase in drag has resulted because of the modifications required for the installation of the ejector.

The thrust-minus-drag ratio of configuration III as a function of the jet pressure ratio is shown in figure 6 for constant values of the cooling-air flow ratio. As for configuration II, the same curves were obtained for all values of tunnel-air velocity showing the thrust-minus-drag ratio to be independent of stream velocity over the range investigated. The pressure distributions were also studied and found to be almost identical to those for configuration II for all values of jet pressure ratio, cooling-air flow, and tunnel-air velocity. The drag coefficient apparently is the same for both configurations.

The curve of zero cooling-air flow ratio shows two sharp breaks, one at a pressure ratio of 2.2 and the other at a pressure ratio of 2.85. These discontinuities and the abruptly lowered values of thrust-minus-drag ratio may well account for a large portion of the performance losses discussed previously. This thrust-minus-drag variation with pressure ratio may be explained in the following manner: The thrust-minus-drag ratio remains relatively constant with pressure ratio increasing from 2.0 to 2.85; at this point the jet overexpands and attaches to the ejector shroud and a system of internal shocks is formed; the pressure in the cooling-air passages is abruptly reduced and a sharp decrease in thrust is noted. Continued pressure ratio increase results in an increase in thrust because the overexpansion of the jet is being decreased. A decrease in the pressure ratio from 4.0 results in obtaining a minimum thrust-minus-drag ratio of 0.80 at a pressure ratio of 2.2 before the jet becomes unattached. The lower value of thrust obtained by decreasing the pressure ratio results from the stability of the shock system and jet attachment once it has formed.

The curves of thrust-minus-drag ratio for cooling-air flow ratios of 0.04 and 0.08 are similar to those shown for configuration II and vary with pressure ratio and cooling-air flow as previously explained for configuration II. As for configuration II it would appear that no large increase in drag has resulted for the modification of configuration I to configuration III.

As mentioned previously, excessive pumping of cooling-air might be another cause of performance loss. The pumping characteristics of configurations II and III are shown in figure 7. The ejector pressure ratio  $P_b/P_j$  (ratio of cooling-air total pressure to jet total pressure) is plotted as a function of the jet pressure ratio for constant values of the cooling-air flow ratio. The cooling-air flow ratios shown are values obtained at the test conditions. These data may be corrected to temperatures corresponding to those of an actual installation by the method of reference 1. For example, a cooling-air flow ratio of 5 percent for the conditions of jet and cooling-air temperature of figure 7(a) represents a cooling-air flow ratio of 6.84 percent at a tail-pipe temperature of  $1600^{\circ}$  R and a cooling-air temperature of  $720^{\circ}$  R.

The pumping characteristics of configuration II (fig. 7(a)) show that for any jet pressure ratio, the cooling-air flow may be increased by increasing the total pressure of the cooling air. For an engine installation using full ram air and operating at constant engine speed and tail-pipe temperature, the ejector-pressure ratio  $P_b/P_j$  will remain nearly constant if the duct pressure ratio  $P_b/P_0$  is constant. The values of  $P_b/P_j$  and  $P_j/p_0$  which would exist if the engine were being operated at the design conditions of flight Mach number and cooling-air flow ratio and with the tail-pipe nozzle open are shown in figure 7(a). At the value of the ejector pressure ratios shown but with the nozzle closed (nonafterburning) the ejector will pump excessively. This value of ejector pressure ratio would probably never be obtained because the duct losses would undoubtedly increase markedly with the increase in cooling-air flow. The actual operating point of any installation will be determined by a balance between the duct pressure losses and the cooling-air flow. In any case, the ejector will pump considerably more than the design value and could cause the losses in performance previously cited because of pressure losses in the internal ducting.

Configuration III shows pumping characteristics similar to those of configuration II, particularly for the higher cooling-air flow ratios (fig. 7(b)). The zero cooling-air-flow-ratio curve shows the same abrupt change indicated on the thrust-minus-drag-ratio curve (fig. 6). The sharp decrease in pressure in the cooling-air passages occurs only for the condition of no cooling-air flow; however, the low values of cooling-air ratio also show a large pressure decrease. The thrust loss for configuration III results from this low-pressure region.

The design point for configuration III is also shown in figure 7(b) and does not indicate excessive pumping. However, for a ram installation operating at a Mach number of 0.9, the pumping will be excessive as it was for configuration II. If configuration III is used in conjunction with a boundary-layer bleed system, which obtains air at free-stream static pressure, the pressure ratios would be somewhat the same as those shown by the dashed curve and would yield a much more satisfactory solution. When used in conjunction with configuration III, such a system will provide satisfactory cooling-air flow at take-off and over the whole range of pressure ratios shown. In addition, the thrust losses for such a system would be small and might well be compensated for by the advantages gained in bleeding off the boundary layer.

Any ejector design which uses full ram air will generally be unsatisfactory at other than the design value. Such an ejector system will either pump too much or too little at conditions other than design.

The thrust and thrust-drag results obtained with configuration IV were nearly the same as those of configuration I. The effect of the partly shrouded exit apparently was negligible as far as the thrust and the drag were concerned, at least for the range of variables investigated.

The pressure distribution on the lower surface of the tail boom is shown in figure 8 for several values of jet pressure ratio. Although the jet is unattached at all values of pressure ratio shown, attachment might occur at higher values of the pressure ratio as indicated by the sharp dip in the expansion region near the exit at high values of pressure ratio.

#### CONCLUDING REMARKS

The modification of configuration I to either of the ejector configurations was accomplished without any large increase in the drag of the body. Two sources of the performance losses occurring under some operating conditions of airplanes equipped with afterburner and cooling-air ejector installations have been identified. The first source results from an overexpansion of the propulsive jet and an internal shock system. This effect, however, only exists at very low cooling-air flow ratios. The second source of performance loss arises from the excessive pumping action resulting from the off-design, that is, non-afterburning operation. Excessive pumping undoubtedly results in large internal duct pressure losses and a consequent momentum deficit.

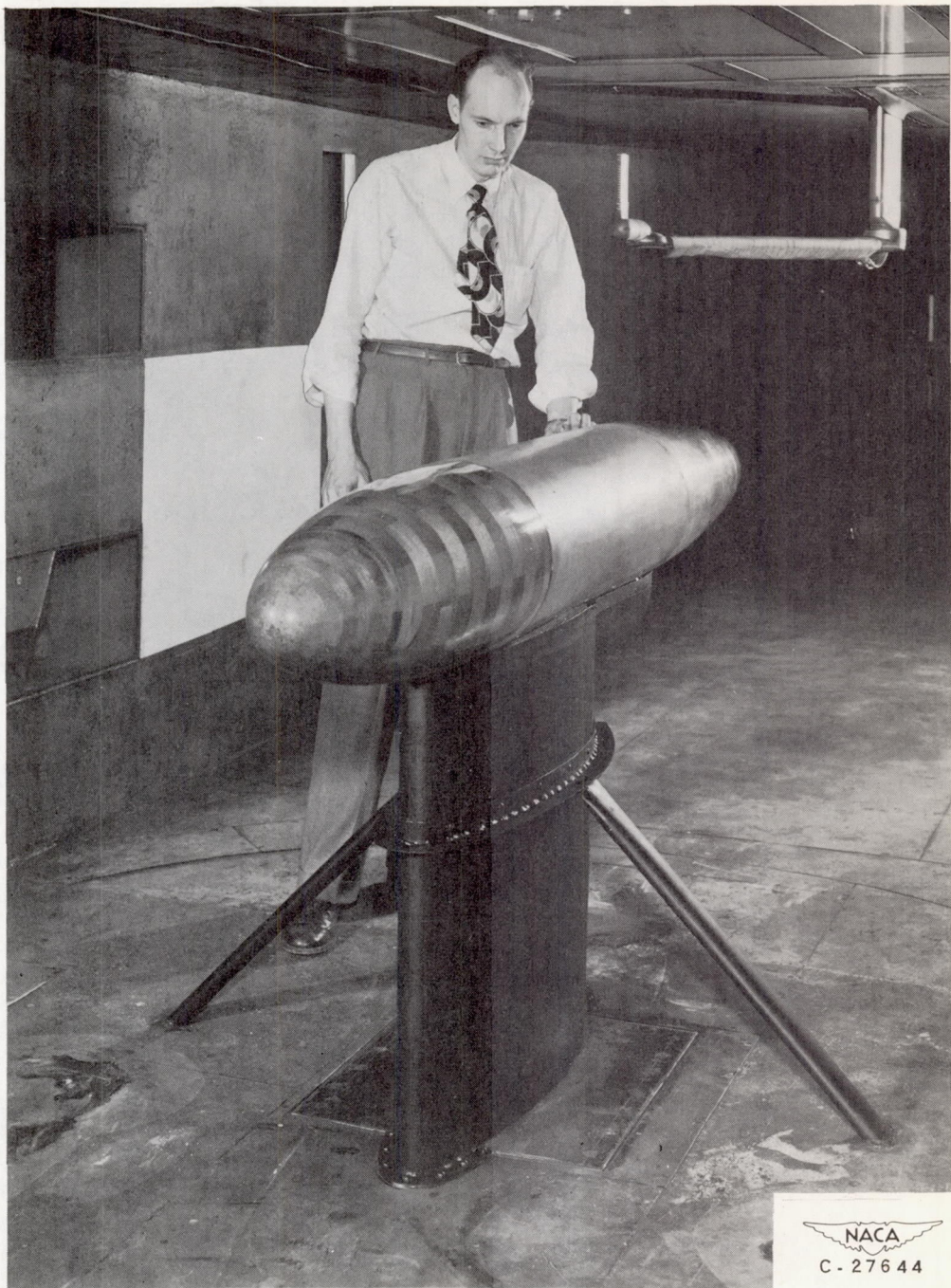
Because a condition of very low cooling-air flow is very unlikely at such off-design ejector operation, the cause of the performance loss in actual installations probably results from excessive duct pressure losses.

The effect of a partial shroud appears negligible as long as the jet remains unattached. The results indicate that, for the model investigated, attachment appears likely at high jet pressure ratios.

Lewis Flight Propulsion Laboratory  
National Advisory Committee for Aeronautics  
Cleveland, Ohio

## REFERENCE

1. Wilsted, H. D., Huddleston, S. C., and Ellis, C. W.: Effect of Temperature on Performance of Several Ejector Configurations. NACA RM E9E16, 1949.



NACA  
C - 27644

Figure 1. - Three-quarter front view of jet-exit model in 6- by 9-foot test section of icing research tunnel.

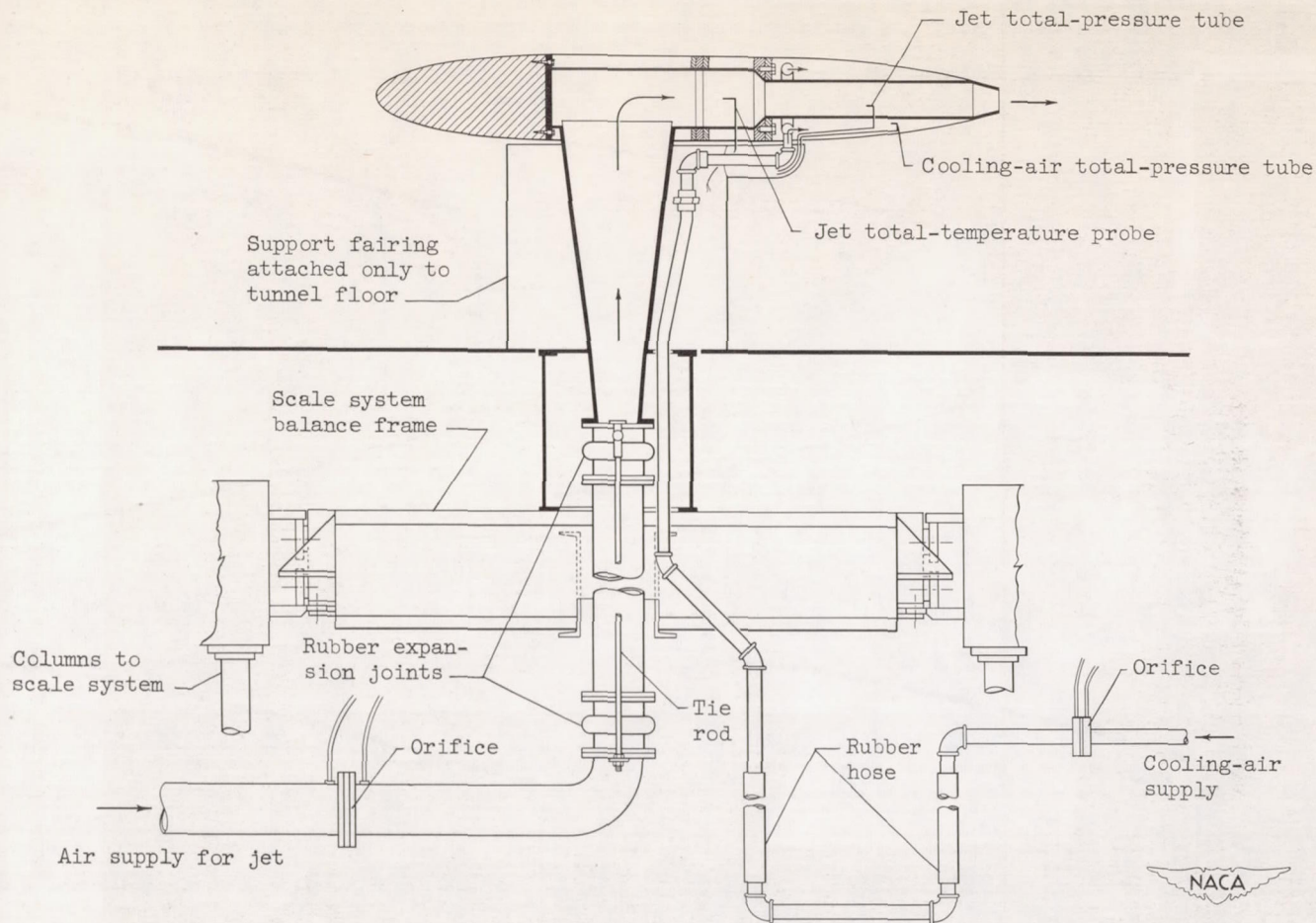
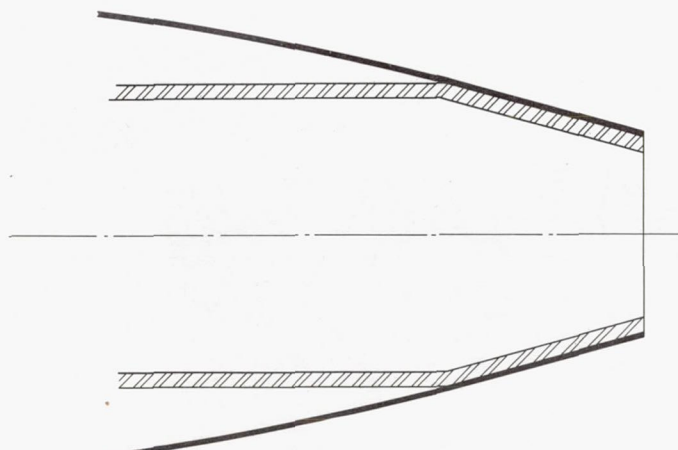
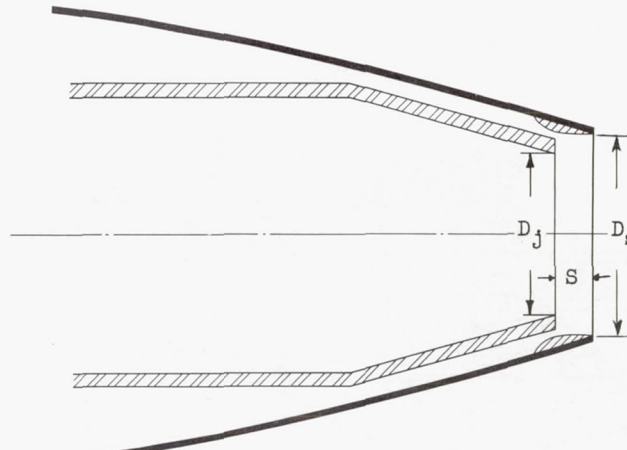


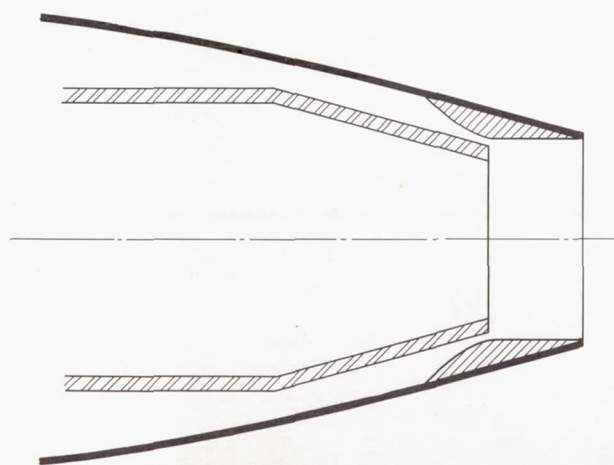
Figure 2. - Schematic diagram of jet-exit model installation and instrumentation in the 6- by 9-foot test section of the icing research tunnel.



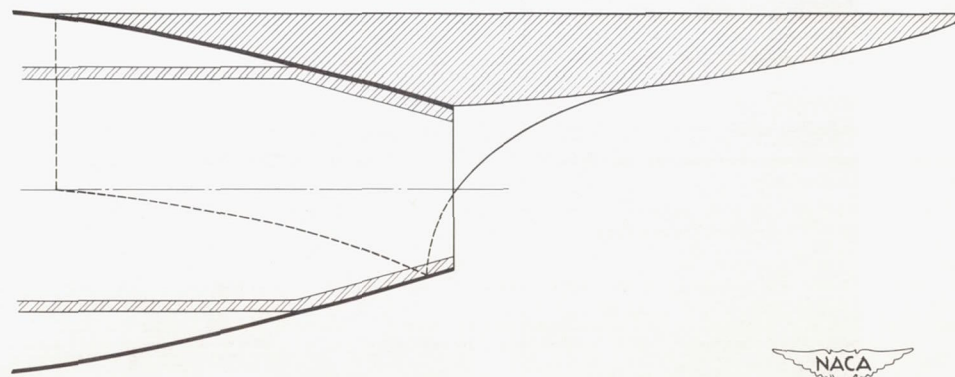
(a) Configuration I.



(b) Configuration II.



(c) Configuration III.



(d) Configuration IV.



Figure 3. - Jet-exit configurations I to IV used in investigation of thrust and drag characteristics. Ratio of shroud to jet diameter, 1.257; ratio of shroud length to jet diameter: configuration II, 0.24; for configuration III, 0.597.

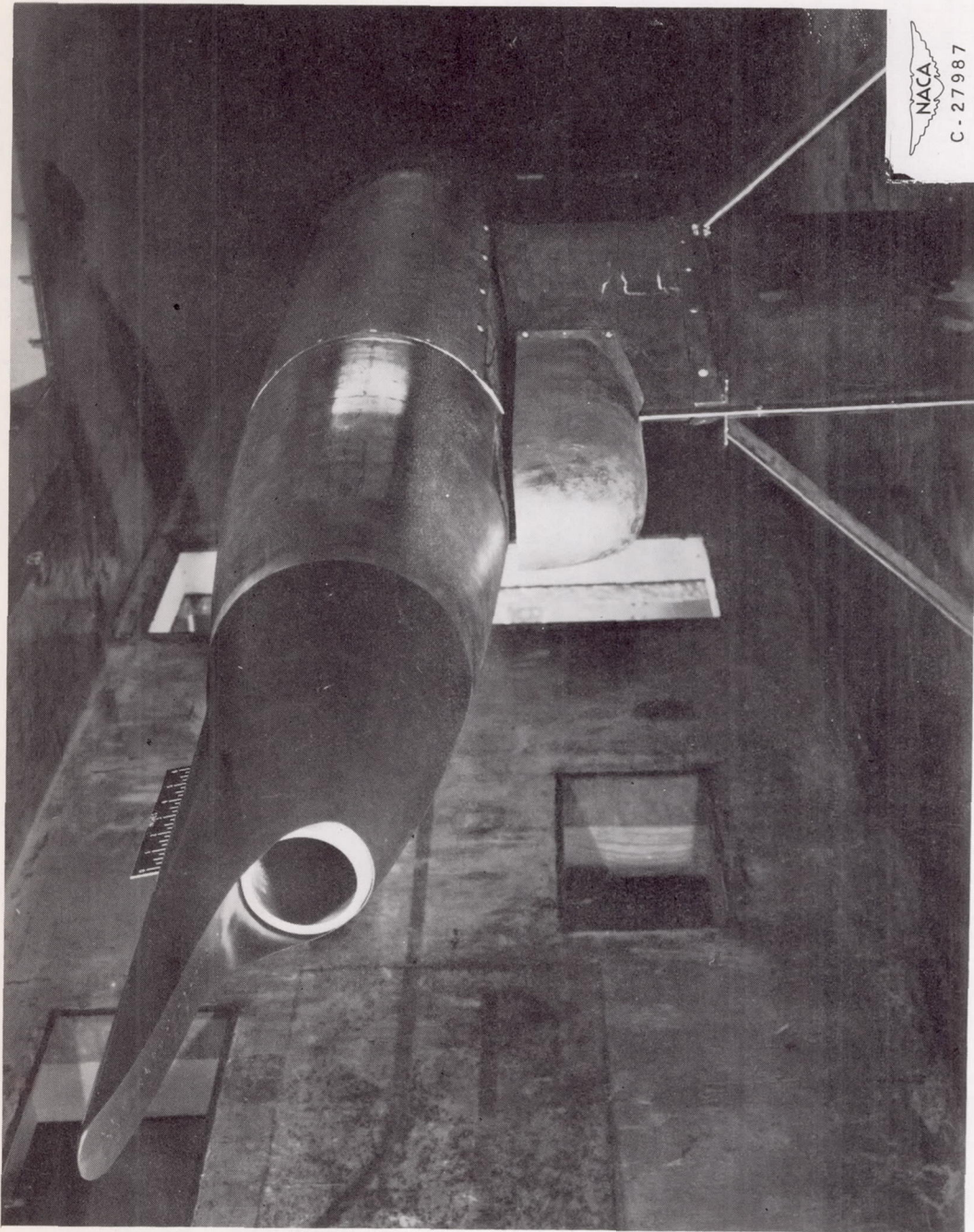


Figure 4. - Three-quarter rear view of jet-exit model configuration IV.

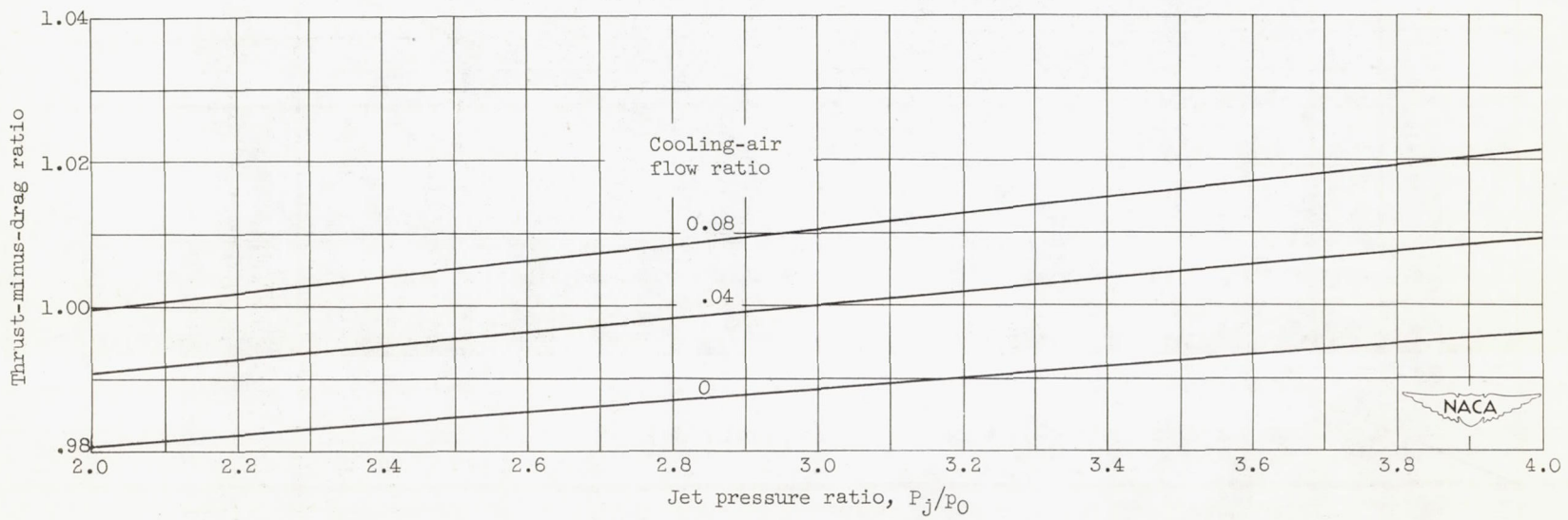


Figure 5. - Ratio of thrust minus drag of configuration II to configuration I as function of jet pressure ratio for three values of cooling-air ratio. Tunnel-air velocity, 305 feet per second.

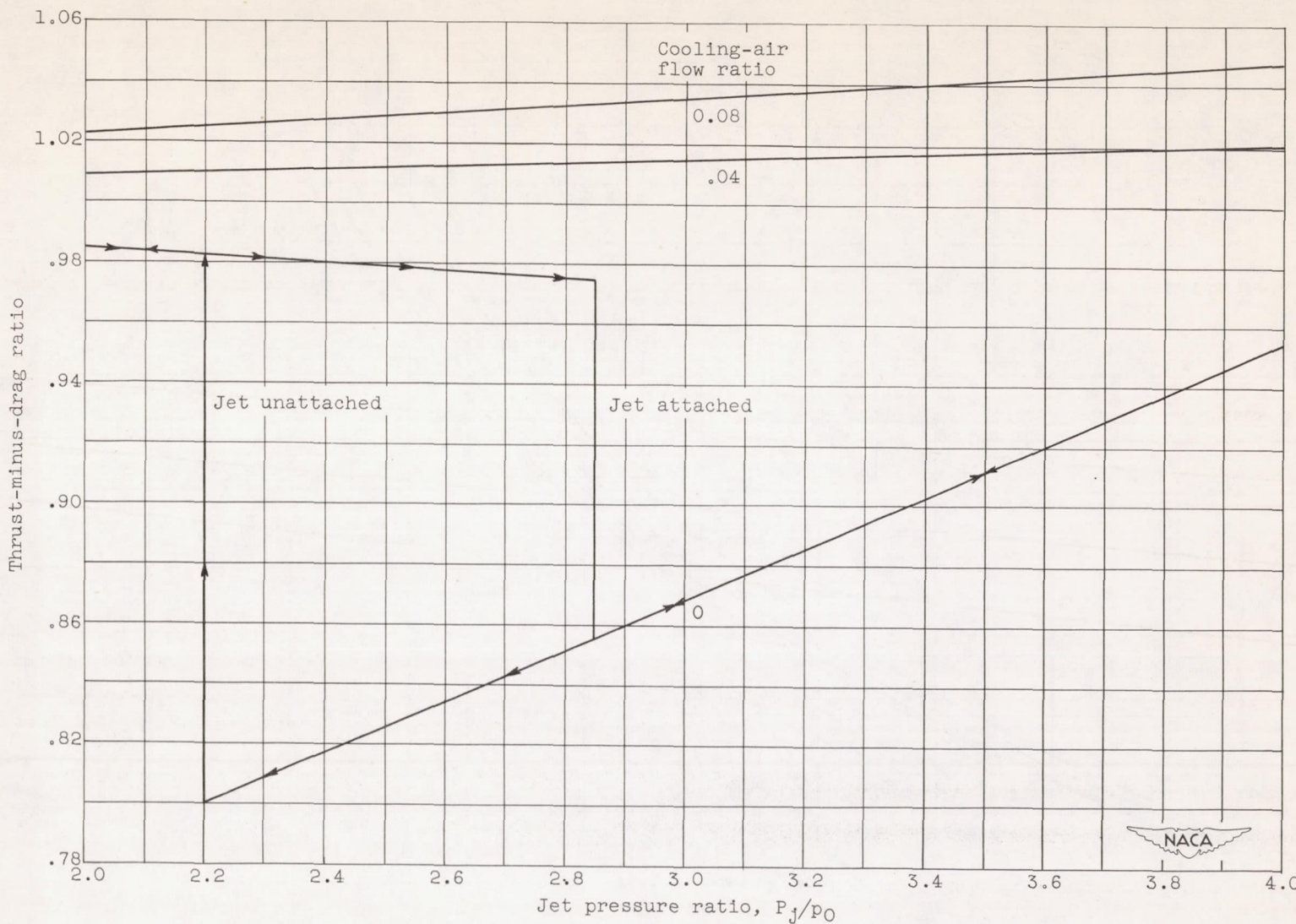
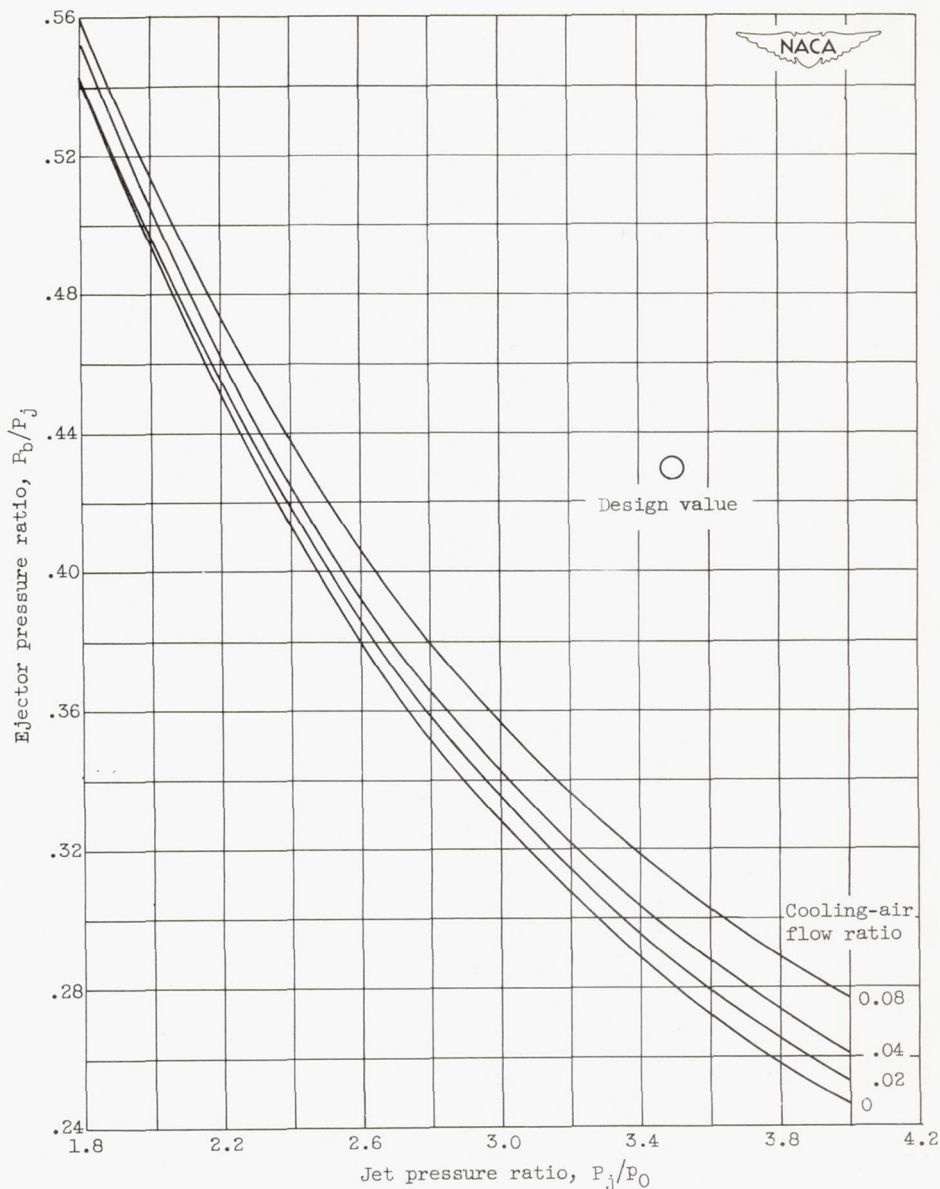
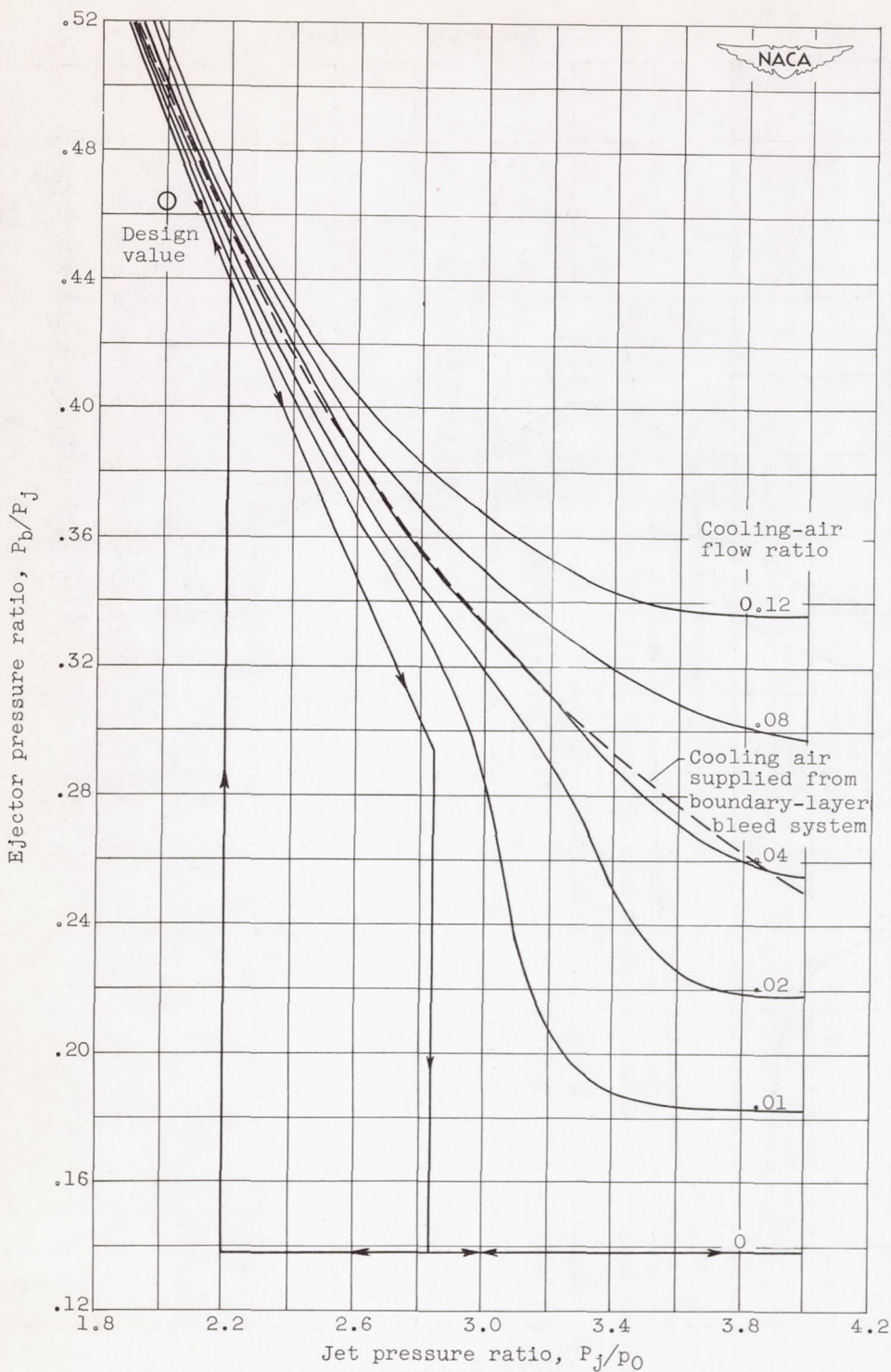


Figure 6. - Ratios of thrust minus drag of configuration III to configuration I as function of jet pressure ratio for three values of cooling-air flow ratio.



(a) Configuration II.

Figure 7. - Pumping characteristics of ejector. Ejector pressure ratio (ratio of cooling-air total pressure to jet-air total pressure) as function of jet pressure ratio for four values of cooling-air flow ratio.



(b) Configuration III.

Figure 7. - Concluded. Pumping characteristics of ejector. Ejector pressure ratio (ratio of cooling-air total pressure to jet-air total pressure) as function of jet pressure ratio for four values of cooling-air flow ratio.

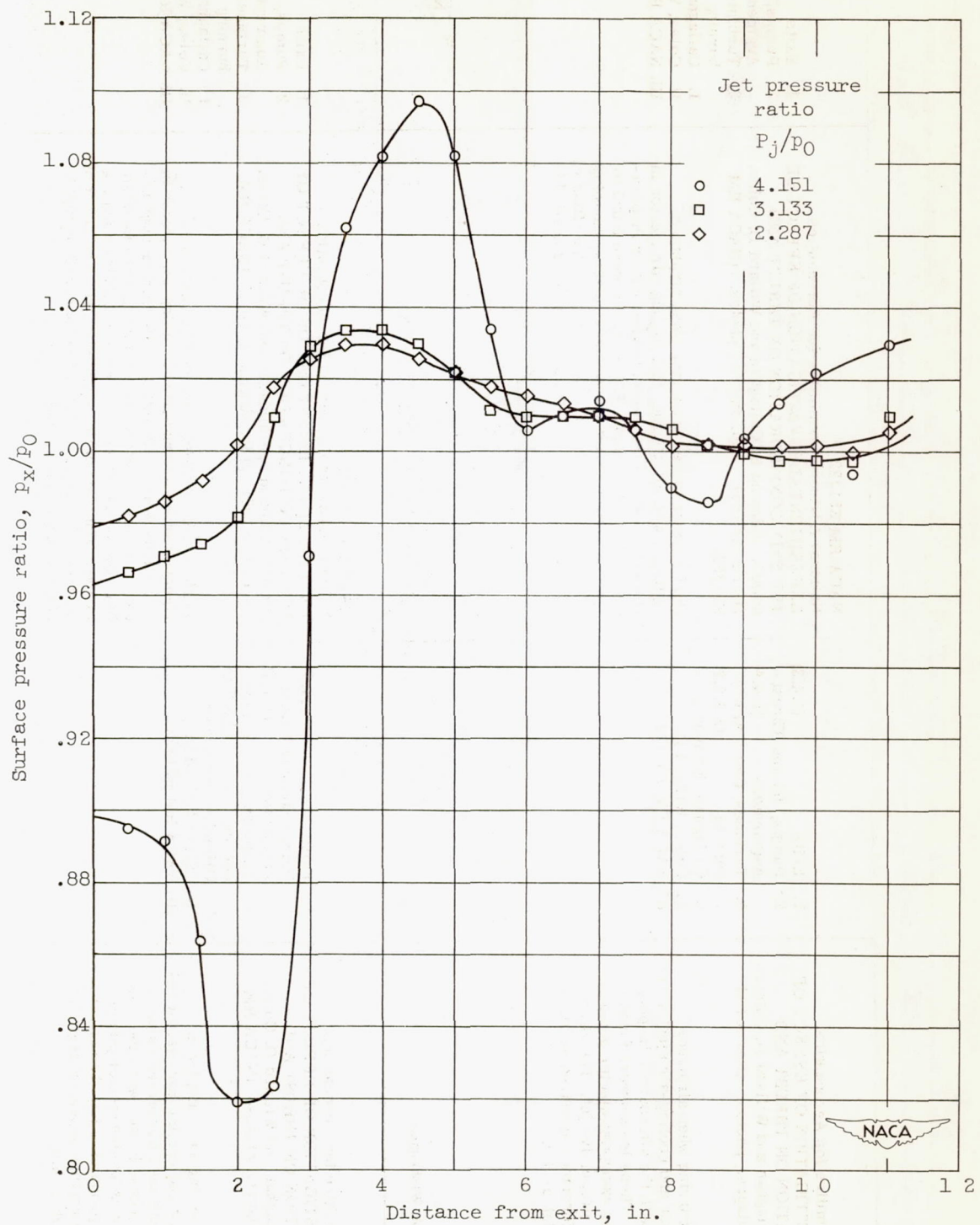


Figure 8. - Effect of jet pressure ratio on static pressures inside tail-boom shroud of configuration IV.